Inorganic Chemistry

ARTICLE

pubs.acs.org/IC

Synthesis of the Clathrate-I Phase $Ba_{8-x}Si_{46}$ via Redox Reactions

Ying Liang,[†] Bodo Böhme,[†] Marianne Reibold,[‡] Walter Schnelle,[†] Ulrich Schwarz,[†] Michael Baitinger,[†] Hannes Lichte,[‡] and Yuri Grin*[,†]

[†]Max-Planck Institute for Chemical Physics of Solids, Nöthnitzer Strasse 40, 01187 Dresden, Germany

[‡]Triebenberg Laboratory, Technical University Dresden, Zum Triebenberg 50, 01328 Dresden, Germany

Supporting Information

ABSTRACT: The clathrate-I phase $Ba_{8-x}Si_{46}$ (space group $Pm\bar{3}n$) was synthesized by oxidation of $Ba_4Li_2Si_6$ with gaseous HCl. Microcrystalline powders of the clathrate phase were obtained within a few minutes. The reaction temperature and the pressure of HCl were optimized to achieve good-quality crystalline products with a composition range of $1.3 < x < 1.9$. The new preparation route presented here provides an alternative to the high-pressure synthesis applied so far.

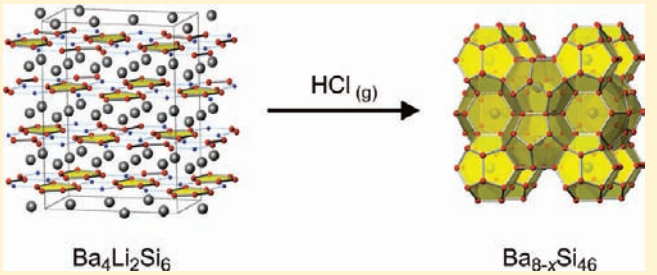

1. INTRODUCTION

At the time when endofullerenes of silicon had been considered as promising candidates for new superconductors, silicon clathrates attracted considerable interest.[1−5] This group of clathrates features polyhedral cages within a covalently bonded silicon network that can be fully, or partially, filled by metal atoms. In the clathrate-I crystal structure of $Ba_{8-x}Si_{46}$, face-sharing dodecahedra Si_{20} $[5^{12}]$ and tetrakaidecahedra Si_{24} $[5^{12}6^2]$ form a space-filling framework. Hitherto, the preparation of superconducting $Ba_{8-x}Si_{46}$ only succeeded under high-pressure conditions starting from $BaSi_2$ and α-Si.[4] Calculations of the specific volume[6] and the ground-state energy[7,8] may explain why $Ba_{8-x}Si_{46}$ favorably forms under high pressure, but its thermodynamic stability with respect to p, T, and x is still under discussion: a comparison of the ground-state energies for $BaSi_2$, α-Si, and Ba_8Si_{46} indicated that the clathrate with fully occupied barium sites is stable only at high pressure.[8] Interestingly, when the high-pressure product $Ba_{7.76}Si_{46}$ was further annealed at 527 °C, a clathrate with lower Ba content, $Ba_{6.63}Si_{46}$, was formed.[4] This result might indicate that the clathrate phase is stable with this composition at ambient pressure. If $Ba_{8-x}Si_{46}$ would form, e.g., from $BaSi_2$ and α-Si in a peritectoid reaction, the formation rate at ambient pressure and temperatures of ≈500 °C would be very low. In a similar case, $BaGe_2$ and α-Ge also do not react to the equilibrium phase $BaGe_5$, which is stable up to ≈550 °C.[9] Hence, to obtain such phases at low temperatures, preparation routes other than annealing are required. A promising alternative method, the oxidation of precursor compounds, was introduced with the preparation of the allotrope Ge($cF136$) in an ionic liquid.[10] Ammonium halides were suggested as oxidizing agents, when clathrate-I $Na_{8-x}Si_{46}$ was found as a crystalline byproduct in the reaction of a mixture of NH_4Br and Na_4Si_4 to amorphous silicon.[11] Clathrate-I phases with enclosed H_2 molecules were later reported to form in reactions between precursor compounds and NH_4Br at 300 °C under dynamic vacuum.[12,13] Using gas−solid reactions, the oxidation method has been further developed and successfully applied for the syntheses of the clathrate-I phases $Na_{6.2}Si_{46}$, K_7Si_{46}, and $Na_2Ba_6Si_{46}$.[14,15] Specifically, the preparation of $Na_2Ba_6Si_{46}$ led to the question of whether $Ba_{8-x}Si_{46}$ can also be prepared by this method. However, our first attempts to oxidize the precursor Ba_3Si_4 by gaseous hydrochloric acid (HCl) to a clathrate phase at temperatures between 350 and 600 °C yielded only $BaCl_2$ and an amorphous product containing mainly silicon.[16] In the present study, we show that clathrate-I $Ba_{8-x}Si_{46}$ can be obtained by oxidation of the precursor phases $Ba_4Li_2Si_6$ and Ba_3Si_4. Furthermore, we present an improved procedure for their controlled reaction with gaseous oxidizing agents.

2. EXPERIMENTAL SECTION

Synthesis. The precursor phase $Ba_4Li_2Si_6$ was obtained by applying the preparation methods given in the literature.[17] NH_4Cl (Merck, p.a.) was dried at room temperature under vacuum ($p < 5 \times 10^{-3}$ mbar) and handled further under argon. To carry out reactions in a single-zone furnace (Figure 1, left), 0.05 mmol of $Ba_4Li_2Si_6$ and 0.85 mmol of NH_4Cl were placed spatially separated in a glass ampule ($V \approx$ 10 mL). Duran ampules were used for reaction temperatures up to 500 °C and quartz ampules for higher temperatures. The ampules were sealed under flowing argon and placed in a preheated furnace. The reaction products were washed with HCl (2 M) and demineralized water to remove the remaining precursor material and metal chlorides. Those products in which the precursor had been completely reacted (according to powder X-ray diffraction, PXRD) did not form gas bubbles while washing. The resulting dark-gray powders were dried under vacuum at

Received: January 26, 2011
Published: April 12, 2011

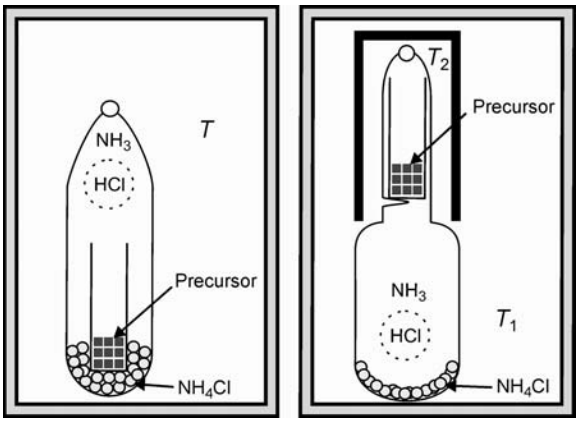

Figure 1. Setup for oxidation of intermetallic compounds by HCl: (left) the precursor and NH_4Cl are placed spatially separated at the same temperature T in a Duran ampule; (right) using a two-zone furnace, the precursor is placed in an open Duran glass in the high-temperature zone (T_2), while NH_4Cl is placed in the low-temperature zone of the ampule (T_1).

room temperature. For reactions that were conducted in two temperature zones, a tube furnace with an additional heating element was used (Reetz). A total of 0.5 mmol of NH_4Cl was placed at the bottom of an ampule with $V \approx 55$ mL (low-temperature zone), and 0.06 mmol of $Ba_4Li_2Si_6$ was deposited in an open Duran glass crucible at the upper part (high-temperature zone; Figure 1, right).

PXRD. The measurements were performed by means of a Guinier Huber G670 camera (image plate, Cu Kα_1 radiation, λ = 1.540 56 Å, graphite monochromator, $5° \leq 2\theta \leq 100°$, $\Delta 2\theta = 0.005°$). Air- and moisture-sensitive samples were fixed between two polyimide foils (7.5 μm, Kapton, Chemplex) on the sample holder. The reflection positions were determined by profile deconvolution of the PXRD pattern and corrected with a LaB_6 standard (a = 4.156 83 Å). Unit cell parameters were calculated from least-squares refinement. Diffraction data for Rietveld refinement were collected with a STOE STADI MP diffractometer [Bragg−Brentano setup, Ge(111) monochromator, Cu Kα_1 radiation, λ = 1.540 56 Å, zero-background holder, $5° \leq 2\theta \leq 119°$, $\Delta 2\theta = 0.02°$]. All crystallographic calculations were performed with the *WinCSD* program package.[18]

Microstructure Analysis. Samples sputtered with gold were investigated with a Philips XL 30 scanning electron microscope (LaB_6 cathode). Energy-dispersive X-ray spectroscopy (EDXS) was performed using an EDAX Si(Li) detector.

Elemental Analysis. For elemental analysis before washing, the samples were heated under vacuum at 200 °C to remove possible residues of NH_4Cl. For analysis after washing, the samples were dried under vacuum at room temperature. In order to measure the barium, lithium, and silicon contents, the samples were dissolved in an aqueous solution of HNO_3/HF. The concentration of the respective element was determined using inductively coupled plasma optical emission spectrometry (Varian VISTA spectrometer). Simultaneous determination of hydrogen, oxygen, and nitrogen was performed using a Leco TCH 600 analyzer. Here, approx. 5 mg of the vacuum-dried sample was put under argon in a tin capsule and transferred in air to the graphite die of the analyzer.

High-Resolution Transmission Electron Microscopy (HRTEM). HRTEM investigations were performed by means of a FEI Tecnai F 20 with Cs correction operated at 200 kV. Finely ground powders were dispersed in ethanol and put on a carbon-hole film.

Magnetic Susceptibility. Magnetization was measured in external fields of 0.002−7 T and in a temperature range from 1.8 to 400 K in a SQUID magnetometer (MPMS XL-7, Quantum Design) on microcrystalline samples ($m \approx 4$−8 mg).

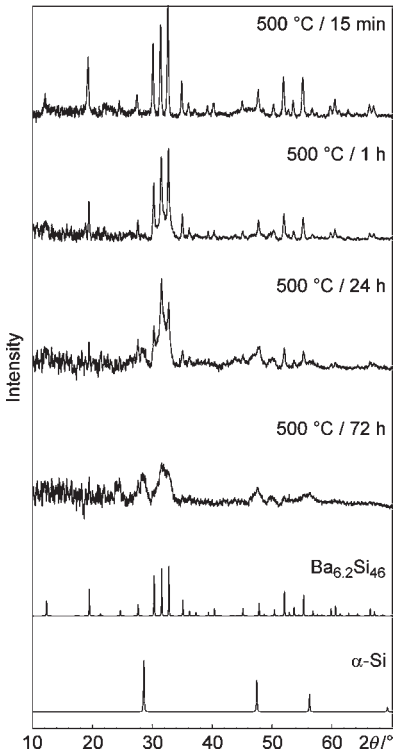

Figure 2. PXRD patterns of the clathrate-I products obtained by oxidation of $Ba_4Li_2Si_6$ at 500 °C for different reaction times in a single-zone furnace. For comparison, simulated diffraction patterns of the clathrate-I $Ba_{6.2}Si_{46}$ and α-Si are given.

Raman Spectroscopy. Raman spectra were obtained at ambient conditions with a Jobin-Yvon (Horiba) LabRam spectrometer equipped with an Olympus optical microscope using a magnification of 50×. For excitation, the blue line of an argon ion laser was used (λ = 488 nm, E = 2.546 eV). The spectral resolution at this wavelength is approximately 4 cm^{-1}; the size of the laser spot is about 10 μm.

3. RESULTS

Reactions in a Single-Zone Furnace. The precursors $Ba_4Li_2Si_6$ and NH_4Cl were heated spatially separated within a sealed Duran ampule (Figure 1, left). At elevated temperatures, NH_4Cl decomposes to gaseous NH_3 and HCl. The PXRD pattern of the product obtained after 15 min of reaction at 500 °C revealed $BaCl_2$ and LiCl, indicating oxidation of the precursor by HCl. After the product was washed, the dark-gray powder showed exclusively reflections of the clathrate-I phase (Figure 2). The crystallinity of the product decreased for longer reaction times at 500 °C. After reaction for 3 days, the clathrate phase had been mostly transformed to an X-ray amorphous product. HRTEM of this product revealed the presence of amorphous material with crystalline nanodomains of α-Si (Figure 3a). At higher reaction temperatures, increasing amounts of α-Si were detected (Figure 4). At 600 °C, the clathrate-I phase was still the main crystalline product after 15 min, but broad reflections of α-Si were also detected. At 700 °C, the PXRD pattern showed mainly broad reflections of α-Si, and the HRTEM images revealed a large fraction of crystalline α-Si domains (Figure 3b). For lower reaction temperatures, the reaction rate strongly decreased. For example, after 30 min at 400 °C, the precursor was still the main

dx.doi.org/10.1021/ic2001859 |*Inorg. Chem.* 2011, 50, 4523–4528

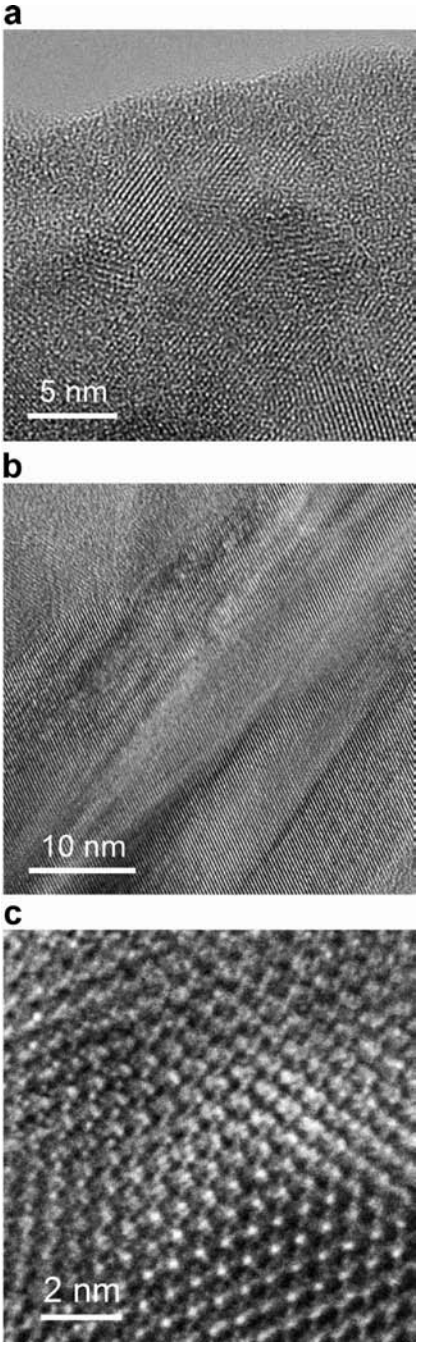

Figure 3. HRTEM images of (a) an amorphous matrix and crystalline nanodomains of α-Si after $Ba_4Li_2Si_6$ was reacted with HCl for 3 days at 500 °C, (b) crystalline domains of α-Si after 15 min at 700 °C, and (c) the clathrate-I phase with composition $Ba_{6.31(1)}Si_{46}$ obtained by reaction in a two-zone furnace (T_1 = 210 °C, T_2 = 400 °C, 3 days), viewed along the [111] direction.

phase in the reaction product. After 1 day at 400 °C, the precursor had been oxidized completely, and after washing, broad reflections of a clathrate-I phase were detected in PXRD. At 300 °C, the precursor was still the main phase after 1 day of reaction.

Reactions in a Two-Zone Furnace. In this arrangement, the precursor $Ba_4Li_2Si_6$ was heated in the hot zone to the reaction temperature T_2, while NH_4Cl was kept at a lower temperature, T_1 (Figure 1, right). In this way, it was possible to investigate the

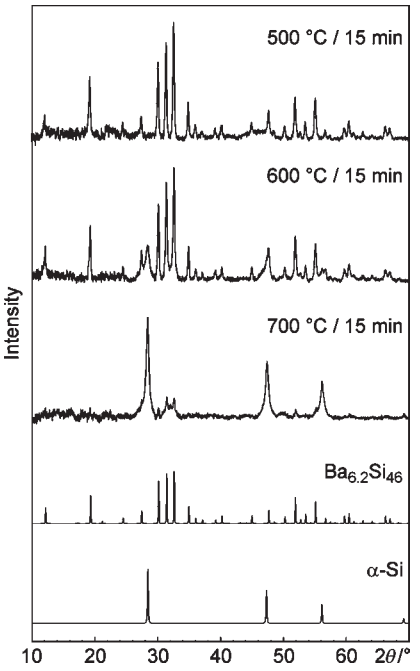

Figure 4. PXRD patterns of the products obtained by oxidation of $Ba_4Li_2Si_6$ at different reaction temperatures in a single-zone furnace. For comparison, simulated diffraction patterns of the clathrate-I $Ba_{6.2}Si_{46}$ and α-Si are given.

oxidation reaction at a given reaction temperature for different partial pressures of HCl. The reaction temperature was adjusted within the range 300 °C ≤ T_2 ≤ 500 °C, while the low-temperature zone was kept at 210 °C ≤ T_1 ≤ 240 °C corresponding to a starting HCl partial pressure of around 7 mbar ≤ p(HCl) ≤ 22 mbar (Table 1). Because NH_4Cl was always found to recrystallize in the low-temperature zone of the ampule, a reservoir of solid NH_4Cl was present during the whole reaction. Hence, the partial pressure of HCl had been determined by the decomposition equilibrium of NH_4Cl[19] at the lower temperature T_1.

After 5 days at T_1 = 210 °C and T_2 = 300 °C, the precursor remained widely unreacted according to PXRD. Also, after washing, a crystalline clathrate phase was not observed. When the reaction temperature was raised to 350 °C ≤ T_2 ≤ 450 °C, only the metal chlorides could be detected by PXRD in the non-washed products after 3 days, while the washed products showed sharp reflections of the clathrate-I phase only (Figure 5a). HRTEM investigations of a typical product $Ba_{6.31(1)}Si_{46}$ (T_1 = 210 °C; T_2 = 400 °C) revealed particles with large crystalline domains of the clathrate-I phase (Figure 3c). Most of the crystallites examined exhibited [110], [111], or [210] orientation, while an orientation along [100] was rarely found. Scanning electron microscopy (SEM) images of this sample indicated clathrate particles of ≈30 μm in size (Figure 6) with composition $Ba_{\sim 5.5}Si_{46}$ according to EDXS. In addition, particles containing only silicon and oxygen were detected. This result is in agreement with elemental analysis, which detected 17 mass % of oxygen, 0.6 mass % of hydrogen, and 5 mass % of nitrogen in the washed product. The high oxygen content is attributed to the washing process, leading to the formation of X-ray amorphous oxides. Before washing, the sample contained only 0.5 mass % of oxygen, 0.2 mass % of hydrogen, and 5 mass % of nitrogen. Because of the presence of

dx.doi.org/10.1021/ic2001859 |*Inorg. Chem.* 2011, 50, 4523–4528

Table 1. Lattice Parameter of $Ba_{8-x}Si_{46}$ Obtained by Oxidation of $Ba_4Li_2Si_6$ in a Two-Zone Furnace[a]

composition	a/Å	reaction conditions[b]
$Ba_{8-x}Si_{46}$[c]	≈10.24	T_1 = 210 °C (p_{HCl} = 6.67 mbar), T_2 = 500 °C, 3 days
$Ba_{8-x}Si_{46}$	10.2520(6)	T_1 = 210 °C (p_{HCl} = 6.67 mbar), T_2 = 450 °C, 3 days
$Ba_{6.18(1)}Si_{46}$	10.2568(5)	T_1 = 240 °C (p_{HCl} = 22.08 mbar), T_2 = 400 °C, 3 days
$Ba_{6.20(1)}Si_{46}$	10.2606(5)	T_1 = 220 °C (p_{HCl} = 10.12 mbar), T_2 = 400 °C, 3 days
$Ba_{6.31(1)}Si_{46}$	10.2701(6)	T_1 = 210 °C (p_{HCl} = 6.67 mbar), T_2 = 400 °C, 3 days
$Ba_{6.62(2)}Si_{46}$	10.2816(6)	T_1 = 210 °C (p_{HCl} = 6.67 mbar), T_2 = 350 °C, 5 days
$Ba_{6.63}Si_{46}$	10.2652(8)	annealing of $Ba_{7.76}Si_{46}$[4]
$Ba_{7.6}Si_{46}$	10.331(2)	high pressure[5]
$Ba_{7.76}Si_{46}$	10.3141(7)	high pressure[4]
Ba_8Si_{46}	10.328(2)	high pressure[3]

[a] Literature data are provided for comparison. [b] The pressure of HCl in mbar was calculated according to the equation: $\log(p_{HCl}) = 9.724 - 4300/T$, where T is the absolute temperature. The equation was derived from the one given by Smits and de Lange for the total equilibrium pressure of NH_4Cl[19] and transformed to mbar units. [c] α-Si (90%) as the main product.

byproduct, the barium and silicon contents of the clathrate phase could not be determined from elemental analysis. However, it was proven that the washed product did not contain lithium (detection limit ≈ 0.1 mass%). Hence, oxidation of $Ba_4Li_2Si_6$ by gaseous HCl (formed by decomposition of NH_4Cl) to the clathrate phase can be described by the following equations:

$$NH_4Cl(s) \rightarrow HCl(g) + NH_3(g)$$

$$23Ba_4Li_2Si_6(s) + (182 + 6x)HCl(g) \rightarrow 3Ba_{8-x}Si_{46}(s) + (68 + 3x)BaCl_2(s) + 46LiCl(s) + (91 + 3x)H_2(g)$$

The yield of the clathrate product is not straightforward to evaluate. Elemental analysis of a washed product containing $Ba_{6.31(1)}Si_{46}$ resulted in a barium content of 14.4 mass%. Assuming that barium is present only in the clathrate phase, the content of $Ba_{6.31(1)}Si_{46}$ in the final product may be ≈36 mass %. As it was mentioned above, the remaining coproducts are amorphous. At higher reaction temperatures (T_2 > 450 °C), α-Si was formed as a byproduct, the amounts of which increased with temperature. After 3 days at 500 °C, the product consisted mainly of α-Si, while only weak reflections of the clathrate-I phase were detected by PXRD.

The conditions that were favorable for oxidation of $Ba_4Li_2Si_6$ to form a crystalline clathrate phase (T_1 = 210 °C; T_2 = 400 °C) were also applied for oxidation of Ba_3Si_4. In contrast to the reactions in a single-zone furnace,[16] a clathrate-I phase was formed albeit with low crystallinity (Figure 5b).

The composition and lattice parameter of $Ba_{8-x}Si_{46}$ obtained from $Ba_4Li_2Si_6$ were determined from PXRD data. The composition ranges from $Ba_{6.18(1)}Si_{46}$ [a = 10.2568(5) Å] to $Ba_{6.62(2)}Si_{46}$ [a = 10.2816(6) Å]. Clathrate products with smaller lattice parameters were observed as well, but the clathrate content in

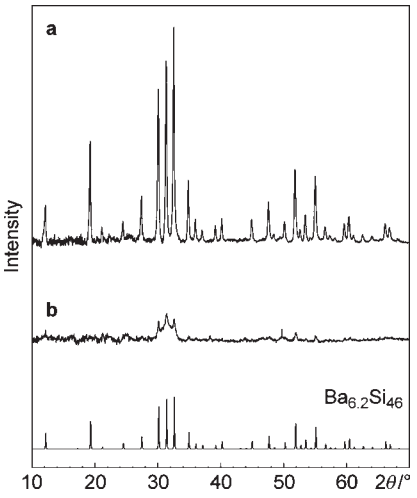

Figure 5. PXRD patterns of the clathrate products obtained by oxidation in a two-zone furnace under the same conditions (T_1 = 210 °C, T_2 = 400 °C, 3 days): (a) using $Ba_4Li_2Si_6$ as the precursor; (b) using Ba_3Si_4 as the precursor. For comparison, the simulated diffraction pattern of $Ba_{6.2}Si_{46}$ is given.

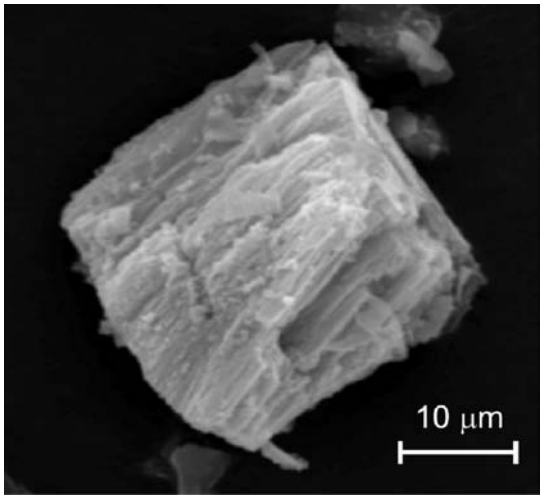

Figure 6. SEM image of an gold-sputtered agglomerate of $Ba_{6.31(1)}Si_{46}$ obtained by oxidation of $Ba_4Li_2Si_6$ in a two-zone furnace (T_1 = 210 °C, T_2 = 400 °C, 3 days).

these samples was too low to allow for a structure refinement (Table 1 and Figure S1 and Tables S1 and S2 in the Supporting Information). The results demonstrate that the barium content of the clathrate phase decreased with an increase in the reaction temperature T_2 and with an increase in the HCl pressure $p_{HCl}(T_1)$.

The barium deficiency in $Ba_{8-x}Si_{46}$ (space group $Pm\bar{3}n$) is caused by a reduced barium occupancy of site 2a in the Si_{20} cages, while the 6d site in the Si_{24} cages was found to be fully occupied by barium. Only for lower barium contents ($x \approx 1.8$) does the refinement point to a small barium deficiency in the Si_{24} cages, which was not considered significant with respect to the estimated experimental errors of a Rietveld refinement. Refinement of the site occupancies and the distances d(Si−Si) (Table S3 in the Supporting Information) indicate the absence of defects in the Si_{46} framework, which are observed in the related germanium compound $Ba_8Ge_{43}\square_3$.[20]

dx.doi.org/10.1021/ic2001859 |Inorg. Chem. 2011, 50, 4523–4528

Superconductivity. From magnetic susceptibility measurements, the reaction products were found to contain superconducting phases with transition temperatures between $T_{c,on}$ = 4.8 K for the $Ba_{6.62(2)}Si_{46}$ sample and $T_{c,on}$ = 3.6 K for the $Ba_{6.18(1)}Si_{46}$ sample (Figure S2 in the Supporting Information). For the $Ba_{6.62(2)}Si_{46}$ sample, the Meissner effect (field cooling) is only 0.6×10^{-3} emu g^{-1}, while the shielding attains 5.8×10^{-3} emu g^{-1} (zero-field cooling). Assuming a density for the clathrate phase of approx. 3.3 g cm^{-3} from our crystal structure refinements, the volume content of the superconducting phase in the product is less than 25%. At high temperatures and fields, all samples were found to be diamagnetic. For products from high-pressure synthesis, a bulk superconductivity with transition temperatures between T_c = 9 K for $Ba_{7.76}Si_{46}$ and T_c = 5 K for $Ba_{6.63}Si_{46}$ was reported.[4]

4. DISCUSSION

The formation of the clathrate-I phase $Ba_{8-x}Si_{46}$ at low pressure and low reaction temperature is a surprising result because this phase has so far only been prepared using high-pressure, high-temperature synthesis. It is evident that the clathrates obtained by oxidation have a lower barium content than the high-pressure products. Considering that a clathrate with lowered barium content was also obtained by annealing the high-pressure product under vacuum,[4] our results point to the thermodynamic stability of $Ba_{8-x}Si_{46}$ at ambient pressure for $x > 1$, at least below 700 °C.

The product formation in oxidation reactions is strongly influenced by the kinetics of the involved reaction steps. Furthermore, under similar reaction conditions, different precursors led to different reaction products: While $Ba_4Li_2Si_6$ was oxidized to the crystalline clathrate-I phase at 500 °C in a single-zone furnace within a reaction time of only 15 min, Ba_3Si_4 was converted under the same conditions to an amorphous product containing mainly silicon.[16] However, it was possible to obtain the clathrate phase from Ba_3Si_4 with optimized reaction conditions in a two-zone furnace, which proves that the presence of lithium is not essential for the formation of the clathrate phase. We attribute the better suitability of $Ba_4Li_2Si_6$ compared with Ba_3Si_4 for the preparation of the clathrate-I phase with high crystallinity to different reaction paths. In the crystal structure of Ba_3Si_4, the silicon atoms form cluster anions Si_4^{6-}, while in $Ba_4Li_2Si_6$, planar Si_6^{10-} rings are linked by lithium atoms to $^2_\infty[Li_2Si_6]^{8-}$ layers separated by barium atoms (Figure 7). Considering the fact that the reaction with HCl proceeds at the surface of the precursor particles, the diffusion rates are crucial for the structural rearrangement involved. The mobility of lithium atoms is much higher than that of barium atoms, allowing for a fast transport of lithium to the particle surface to form chloride. Removal of lithium atoms from the precursor induces the formation of Si−Si bonds, which leads to the further encapsulation of barium atoms and hinders their reaction to $BaCl_2$. To form a crystalline clathrate phase, the reaction temperature has to be high enough to allow for structural rearrangements, but the oxidation rate has to be sufficiently low to prevent barium atoms to be removed from the substrate, which can be achieved by a low partial pressure of HCl. However, in the case of NH_4Cl as the HCl source, both parameters could be varied independently only in a two-zone furnace, in which the partial pressure of HCl was controlled by the temperature T_1 of the NH_4Cl source (Figure 1, right). For higher reaction temperatures (i.e., higher reaction rates) and for higher HCl partial pressures, the barium

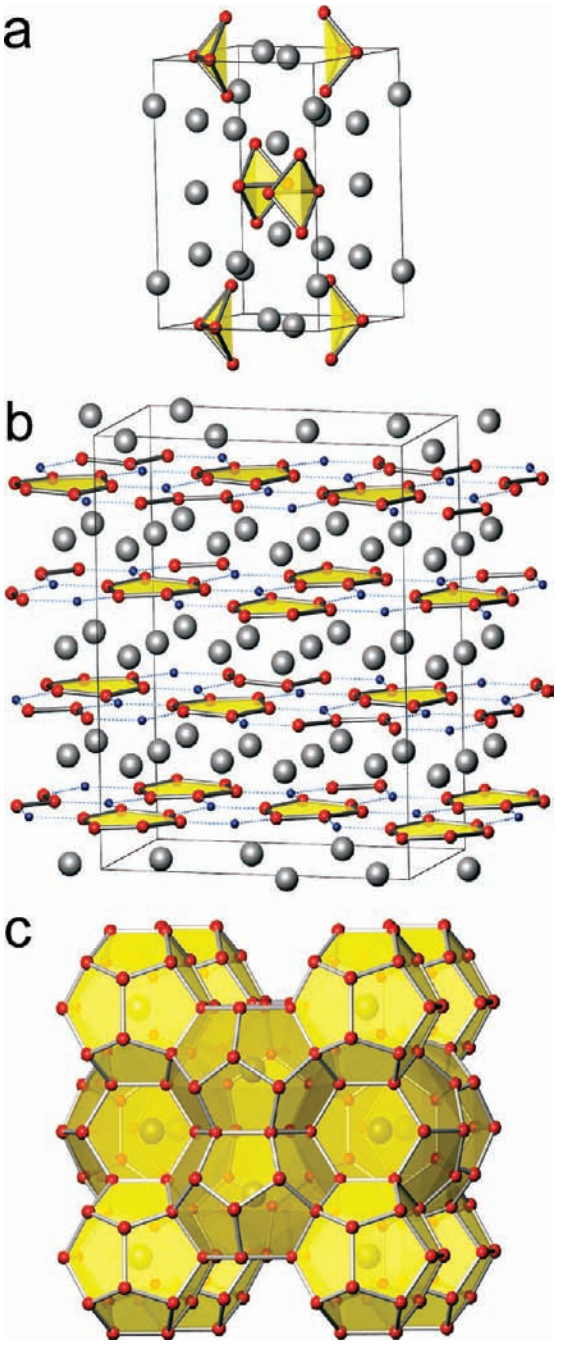

Figure 7. Crystal structures of (a) Ba_3Si_4, (b) $Ba_4Li_2Si_6$, and (c) clathrate-I $Ba_{8-x}Si_{46}$. Silicon atoms are drawn in red (medium size), barium atoms in gray (large), and lithium atoms in blue (small).

content in the clathrate phase was reduced (Table 1). With an increase in the reaction time, the clathrate phase was found to be further oxidized by HCl to nanocrystalline α-Si or amorphous phases. In order to achieve a high yield of the clathrate phase, the reaction time has to be optimized with respect to the reaction conditions applied.

Because hydrogen was found in the reaction product by elemental analysis, a possible encapsulation of hydrogen in the clathrate framework was investigated. Distinct amounts of molecular hydrogen had been also reported for a silicon clathrate with composition $Na_{5.5}(H_2)_{2.15}Si_{46}$.[12] From PXRD data, the

dx.doi.org/10.1021/ic2001859 |*Inorg. Chem.* 2011, 50, 4523–4528

silicon positions in the framework and the barium positions within the large Si_{24} cages were refined with full occupancy. Because of the large scattering contrast of hydrogen to the other elements, the presence of hydrogen atoms or molecules at this site can be ruled out. However, the smaller Si_{20} cages are found to be only partially occupied by barium, so that the presence of hydrogen atoms or molecules at this site cannot be excluded by X-ray diffraction. Because hydrogen is more electronegative than silicon, an isolated atom in the Si_{20} cage should be a hydride anion. Mixed occupancy of clathrate cage sites by cations and anions (and this has to be assumed for Ba^{2+} and H^-) is highly unlikely and has so far not been reported. To check for the presence of hydrogen molecules in the sample, Raman measurements were performed. As a result, neither the stretching vibrations of molecular hydrogen around 4156 cm^{-1}[21] nor the vibrations of Si−H bonds at around 2100 cm^{-1} were detected (Figure S3 in the Supporting Information). Thus, taking into account also the results of elemental analysis, we attribute the presence of hydrogen in the reaction product to hydroxyl and amide groups on the particle surface or within the X-ray amorphous byproduct. The presence of nitrogen in the clathrate structure is unlikely as well because a substitution of silicon atoms by nitrogen atoms within the framework would further increase the occupancy of antibonding states. Substantial amounts of nitrogen should be detected in the structure refinement. Furthermore, if nitrogen would be a part of the clathrate structure, its relative amount should increase upon washing of the sample. This is clearly not the case.

5. CONCLUSION

The preparation of the clathrate-I phase $Ba_{8-x}Si_{46}$ by oxidation of $Ba_4Li_2Si_6$ provides an alternative route to the high-pressure synthesis used so far. Because high-pressure preparations are complex and limited to small amounts of reaction products, an alternative route is of general interest. The yield and crystallinity of the clathrate phase obtained by the oxidation reaction were optimized by tuning reaction temperature and pressure of HCl independently. With NH_4Cl as the HCl source, the reaction conditions could be conveniently controlled using a two-zone furnace. Complex rearrangements of the silicon atoms during the oxidation reactions can proceed within a short time at comparatively low temperatures. The formation of $Ba_{8-x}Si_{46}$ at low pressure would be in agreement with a thermodynamic existence field of the phase at ambient pressure.

■ ASSOCIATED CONTENT

Supporting Information. Crystallographic information files (CIF), crystallographic data, PXRD patterns, supplemental figures, and safety information. This material is available free of charge via the Internet at http://pubs.acs.org.

■ AUTHOR INFORMATION

Corresponding Author
*E-mail: grin@cpfs.mpg.de.

■ ACKNOWLEDGMENT

The authors thank P. Scheppan, R. Koban, and the Kompetenzgruppe Struktur. M.B., M.R., H.L., and Yu.G. gratefully acknowledge financial support from the Deutsche Forschungsgemeinschaft (SPP 1415, "Kristalline Nichtgleichgewichtsphasen (KNG)-Präparation, Charakterisierung und in situ-Untersuchung der Bildungsmechanismen"). B.B. and Yu.G. gratefully acknowledge funding by the European Union and the Free State of Saxony (SAB Project 13853/2379).

■ REFERENCES

(1) Tanigaki, K.; Shimizu, T.; Itoh, K. M.; Teraoka, J.; Moritomo, Y.; Yamanaka, S. *Nat. Mater.* **2003**, *2*, 653–655. Yamanaka, S. *Dalton Trans.* **2010**, *39*, 1901–1915.
(2) Yamanaka, S.; Horie, H.-O.; Nakano, H.; Ishikawa, M. *Fullerene Sci. Technol.* **1995**, *3*, 21–28. Kawaji, H.; Horie, H.-O.; Yamanaka, S.; Ishikawa, M. *Phys. Rev. Lett.* **1995**, *74*, 1427–1429.
(3) Yamanaka, S.; Enishi, E.; Fukuoka, H.; Yasukawa, M. *Inorg. Chem.* **2000**, *39*, 56–58.
(4) Fukuoka, H.; Kiyoto, J.; Yamanaka, S. *Inorg. Chem.* **2003**, *42*, 2933–2937.
(5) Fukuoka, H.; Kiyoto, J.; Yamanaka, S. *J. Solid State Chem.* **2003**, *175*, 237–244.
(6) Wilson, M.; McMillan, P. F. *Phys. Rev. Lett.* **2003**, *90*, 135703.
(7) Imai, M.; Kikegawa, T. *Inorg. Chem.* **2008**, *47*, 8881–8883.
(8) Imai, Y.; Watanabe, A. *Intermetallics* **2010**, *18*, 542–547.
(9) Aydemir, U.; Akselrud, L.; Carrillo-Cabrera, W.; Candolfi, C.; Oeschler, N.; Baitinger, M.; Steglich, F.; Grin, Y. *J. Am. Chem. Soc.* **2010**, *132*, 10984–10985.
(10) Guloy, A. M.; Ramlau, R.; Tang, Z.; Schnelle, W.; Baitinger, M.; Grin, Yu. *Nature* **2006**, *443*, 320–323.
(11) McMillan, P. F.; Gryko, J.; Bull, C.; Arledge, R.; Kenyon, A. J.; Cressey, B. A. *J. Solid State Chem.* **2005**, *178*, 937–949.
(12) Neiner, D.; Okamoto, N. L.; Condron, C. L.; Ramasse, Q. M.; Yu, P.; Browning, N. D.; Kauzlarich, S. M. *J. Am. Chem. Soc.* **2007**, *129*, 13857–13862.
(13) Neiner, D.; Okamoto, N. L.; Yu, P.; Leonard, S.; Condron, C. L.; Toney, M. F.; Ramasse, Q. M.; Browning, N. D.; Kauzlarich, S. M. *Inorg. Chem.* **2010**, *49*, 815–822.
(14) Böhme, B.; Guloy, A.; Tang, Z.; Schnelle, W.; Burkhardt, U.; Baitinger, M.; Grin, Yu. *J. Am. Chem. Soc.* **2007**, *129*, 5348–5349.
(15) Böhme, B.; Aydemir, U.; Ormeci, A.; Schnelle, W.; Baitinger, M.; Grin, Yu. *Sci. Technol. Adv. Mater.* **2007**, *8*, 410–415.
(16) Aydemir, U.; Ormeci, A.; Borrmann, H.; Böhme, B.; Zürcher, F.; Uslu, B.; Goebel, T.; Schnelle, W.; Simon, P.; Carrillo-Cabrera, W.; Haarmann, F.; Baitinger, M.; Nesper, R.; von Schnering, H. G.; Grin, Yu. *Z. Anorg. Allg. Chem.* **2008**, *634*, 1651–1661.
(17) von Schnering, H. G.; Bolle, U.; Curda, J.; Peters, K.; Carrillo-Cabrera, W.; Somer, M.; Schultheiss, M.; Wedig, U. *Angew. Chem., Int. Ed. Engl.* **1996**, *35*, 984–986.
(18) Akselrud, L. G.; Zavalii, P. Yu.; Grin, Yu.; Pecharsky, V. K.; Baumgartner, B.; Wölfel, E. *Mater. Sci. Forum* **1993**, *133−136*, 335–340.
(19) Smits, A.; de Lange, W. *J. Chem. Soc.* **1928**, 2944–2952.
(20) Aydemir, U.; Candolfi, C.; Borrmann, H.; Baitinger, M.; Ormeci, A.; Carrillo-Cabrera, W.; Chubilleau, C.; Lenoir, B.; Dauscher, A.; Oeschler, N.; Steglich, F.; Grin, Yu. *Dalton Trans.* **2010**, *39*, 1078–1088.
(21) Brodsky, M. H.; Cardona, M.; Cuomo, J. J. *Phys. Rev. B* **1977**, *16*, 3556–3571.